

High- Q MgF_2 whispering gallery mode resonators for refractometric sensing in aqueous environment

Florian Sedlmeir^{1,2,3,†*} and Richard Zeltner^{1,2,†}, Gerd Leuchs^{1,2}, and Harald G.L. Schwefel^{1,2}

¹ *Max Planck Institute for the Science of Light,
Günther-Scharowsky-Straße 1/Building 24, 91058 Erlangen, Germany*

² *Friedrich-Alexander-Universität Erlangen-Nürnberg (FAU),
Department of Physics, Institute for Optics, Information and Photonics,
Staudtstr.7/B2, 91058 Erlangen, Germany and*

³ *SAOT, School in Advanced Optical Technologies,
Paul-Gordan-Str. 6, 91052 Erlangen, Germany*

[†] *authors contributed equally*

We present our experiments on refractometric sensing with ultrahigh- Q , crystalline, birefringent magnesium fluoride (MgF_2) whispering gallery mode resonators. The difference to fused silica which is most commonly used for sensing experiments is the small refractive index of MgF_2 which is very close to that of water. Compared to fused silica this leads to more than 50% longer evanescent fields and a 4.25 times larger sensitivity. Moreover the birefringence amplifies the sensitivity difference between TM and TE type modes which will enhance sensing experiments based on difference frequency measurements. We estimate the performance of our resonators and compare them with fused silica theoretically and present experimental data showing the interferometrically measured evanescent decay and the sensitivity of mm-sized MgF_2 whispering gallery mode resonators immersed in water. They show reasonable agreement with the developed theory. Furthermore, we observe stable Q factors in water well above 1×10^8 .

* florian.sedlmeir@mpl.mpg.de

I. INTRODUCTION

Whispering gallery mode (WGM) resonators have been established as a powerful tool for various sensing application over the last decade. Such dielectric resonators confine light via total internal reflection close to their surface causing an evanescent field leaking out into the environment. The resulting high- Q resonances are thus sensitive to parameter changes of the resonator itself as well as of the surrounding. The applications range from refractometric sensing [11, 29], temperature [10] and pressure sensing [14, 28] to the detection of nearly any kind of biological matter like viruses, microorganisms and proteins [2, 20, 25] even down to the single molecule level [4, 26].

The most common types of WGM resonators used for sensing are fused silica microspheres [2], silica microtoroids [13] and polystyrene microbeads [18]. These devices share isotropic optical properties, high refractive indices compared to water and their amorphous nature. In this study we introduce and investigate for the first time ultrahigh- Q single crystal WGM resonators for sensing purposes. We chose magnesium fluoride (MgF_2) as the resonator material because its refractive index is very close to that of water and it is thus expected to show a stronger sensitivity towards the surrounding. Moreover it is slightly anisotropic and therefore the difference in responsivity of TM and TE modes is larger than in isotropic materials which will help to implement schemes based on relative frequency measurements. Finally MgF_2 resonators are known for their high Q factors [1, 16], which do not degraded in aqueous environment [24], apart from the influence of potential absorption of the evanescent field by water.

In the first part of the paper we discuss the differences concerning sensitivity, behavior of TM and TE modes and evanescent field length between fused silica and MgF_2 resonators theoretically. In the second part we present experimental results showing the significantly extended evanescent field decay length and sensitivities against refractive index changes of two different MgF_2 WGM resonator geometries.

II. THEORY

Whispering gallery modes have been analytically described for different geometries in various publications [3, 5, 8, 19, 22]. Such modes arise from boundary conditions at the rim of convex shaped, usually rotationally symmetric, dielectric bodies like spheres or spheroids. Due to the resonator's higher refractive index compared with the surrounding, the light can be guided and confined via total internal reflection at the boundary. Geometry and material properties determine the resonance positions of the different types of modes. Usually these modes can be characterized by the three mode numbers l, q, p which correspond to different intensity distributions of the light close to the boundary: $q \in \mathbb{N}$ counts the number of maxima in radial direction, $p + 1 \in \mathbb{N}$ corresponds to the number of maxima in polar direction and $l - p$ is the number of field oscillations along one roundtrip around the cavity. For close to fundamental modes l can be estimated sufficiently with $l \approx 2\pi R n_r / \lambda_0$.

The spectral position of the modes are found by solving Maxwell's equations under proper boundary conditions. They depend on the mode numbers, the refractive index of the resonator n_r and its radius R as well as the index of the surrounding n_s . For refractometric sensing, we are interested in the dependence of the resonance wavelengths on small changes of n_s , which can be easily calculated by taking the derivative of the modal dispersion relation

(see Ref. [11]). This yields for a spherical geometry

$$\frac{\partial}{\partial n_s} \lambda_{l,q}^{(TE)} = \frac{\lambda^2}{2\pi R} \frac{n_s}{(n_r^2 - n_s^2)^{3/2}} \left[1 - \frac{\zeta_q}{2^{1/3}} \frac{n_r^2}{n_r^2 - n_s^2} \left(l + \frac{1}{2} \right)^{-2/3} \right], \quad (1)$$

$$\begin{aligned} \frac{\partial}{\partial n_s} \lambda_{l,q}^{(TM)} = & \frac{\lambda^2}{2\pi R} \frac{n_s}{n_r^2 (n_r^2 - n_s^2)^{3/2}} \left[2n_r^2 - n_s^2 \right. \\ & \left. - \frac{\zeta_q}{2^{1/3}} \frac{2n_r^6 + n_r^4 n_s^2 - 4n_r^2 n_s^4 + 2n_s^6}{n_r^2 (n_r^2 - n_s^2)} \left(l + \frac{1}{2} \right)^{-2/3} \right] \end{aligned} \quad (2)$$

The superscript denotes the polarization, where TE corresponds to modes with electric field vectors parallel to the surface and TM perpendicular to it. Due to different boundary conditions the two polarizations have slightly different sensitivities, even for isotropic resonator materials such as fused silica. Note that there is no dependence on the mode number p . This degeneracy is a consequence of the radial symmetry of a perfect sphere and is usually not observed in experiments due to imperfections in the fabrication process of the resonator. If the deviation from a sphere is strong, which is commonly the case for mechanically produced crystalline WGM resonators, the $p \neq 0$ modes have to be described by a slightly modified dispersion relation which can be found in [3, 5, 8]. These equations contain terms depending on the eccentricity which, however, do not depend on the index of refraction and therefore cancel out when taking the derivative. Thus we conclude that Eq. (1) and (2) predict the sensitivity of non spherical resonators satisfactorily.

For the following considerations we always assume fundamental modes with $q = 1$ and $p = 1$, however, it is worth mentioning that the sensitivity increases by approximately 2 – 3% per increased q -number. Apart from that, the sensitivity is mainly determined by the refractive index difference between the resonator and the surrounding $n_r^2 - n_s^2$ and the radius R . This is illustrated in Fig. 1 where Eq. (1) and (2) are plotted for different geometries and materials. In Fig. 1(a) the index of the surrounding is assumed as $n_s = 1.329$ (water at 795 nm) and the sensitivity is plotted against the index of the resonator n_r . It is apparent that the sensitivity increases significantly when n_r approaches n_s . The plot also shows that the performance of MgF_2 is in general better than fused silica due to its smaller refractive index. In addition MgF_2 is slightly birefringent ($n_o = 1.375$, $n_e = 1.387$, see [6]), hence the difference between TE and TM modes (corresponding to extraordinary and ordinary polarization in a z -cut resonator) is stronger than in isotropic fused silica. In Fig. 1(b) we plot the sensitivity against the resonator radius for MgF_2 and fused silica for both polarizations. The double logarithmic plot reveals that the sensitivity scales nearly inversely proportional for all cases down to very small resonator sizes. Therefore we find, that a MgF_2 resonator can be 4.25 times larger than a fused silica one to show the same sensitivity against refractive index change. It is interesting to mention, that the ratio of shifts between TM and TE modes is also nearly constant for all cases. They are 1.17 for fused silica and 1.49 for MgF_2 WGM resonators.

The higher sensitivity of MgF_2 has certain advantages over fused silica. As the resonator can be approximately four times larger to provide the same performance, a mechanically stable implementation is much easier. Also, larger resonators show less noise due to thermally induced short term fluctuations. Significant contributions come either from thermoelasticity or thermorefraction which scale inversely proportional to the resonator volume and the modal

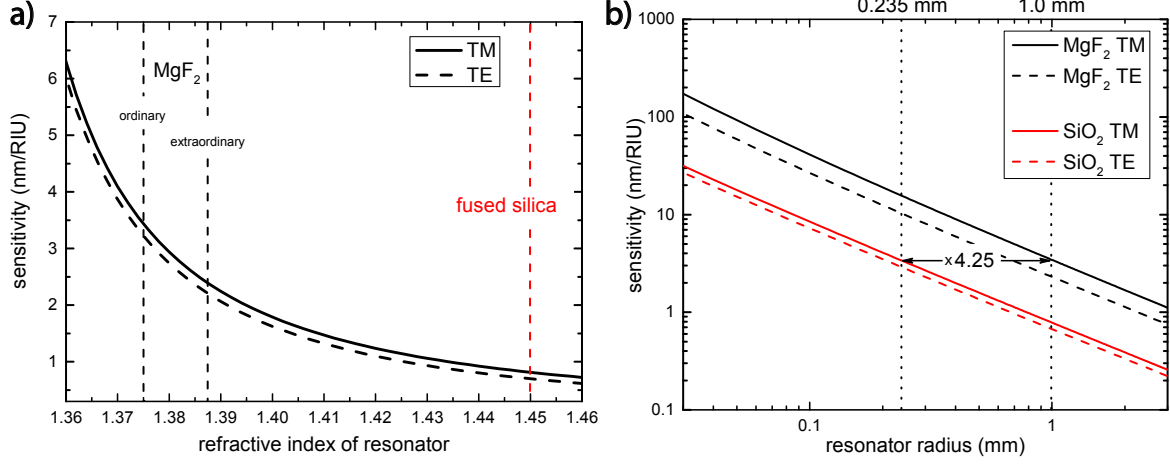


FIG. 1: a) shows the dependence of the sensitivity (wavelength change of the modes over refractive index unit (RIU) change) on the bulk index of the used resonator material. The resonator radius was assumed to be $R = 1$ mm and we only consider fundamental modes ($q = 1$). TM and TE modes have slightly different sensitivities due to different boundary conditions, but both increase when the resonator index comes closer to the index of the surrounding (which is assumed to be water, $n_s = 1.329$ at 795 nm). The refractive indices of MgF₂ and fused silica are marked by dashed lines. It is apparent that the birefringence of MgF₂ causes a stronger dispersion between TE and TM as compared to the isotropic cases such as fused silica. b) shows the sensitivities of MgF₂ and fused silica resonators against their radius. The linearity in the double logarithmic plot indicates that MgF₂ resonators can always be 4.25 times larger to reach the same sensitivity as fused silica ones. Moreover the ratio between TM and TE sensitivities stays constant (nameley 1.49 for MgF₂ and 1.17 for fused silica).

volume respectively [7, 21]. However, we want to point out, that long term thermal drifts, which are the major problem in most resonator based sensing applications are independent of the resonator size and arise only from material parameters such as thermal expansion and thermorefraction. These are very similar to those of fused silica and thus thermal drifts are expected to be in the same order of magnitude. To overcome this problem, Le et al. [15] proposed and demonstrated a scheme using difference frequency measurements between TE and TM modes in fused silica. As this difference is significantly more sensitive to refractive index changes than to temperature changes, the influence of thermal drifts has been reduced. Such a scheme requires high enough modal density, to observe TE and TM modes within the sweeping range of the laser simultaneously, and the difference between the TE and TM sensitivities being as large as possible. Both is given in MgF₂ resonators due to the larger resonator size and the materials birefringence.

Finally, we want to point out that the small index contrast of MgF₂ with respect to water results in a significantly longer decay distance of the evanescent field leaking out of the cavity. The field decay outside the dielectric $r > R$ can be described as [17]

$$E(r) \propto e^{-\kappa r} \quad \text{with} \quad \kappa \approx \frac{2\pi}{\lambda_0} \sqrt{n_{\text{eff}}^2 - n_s^2} \quad (3)$$

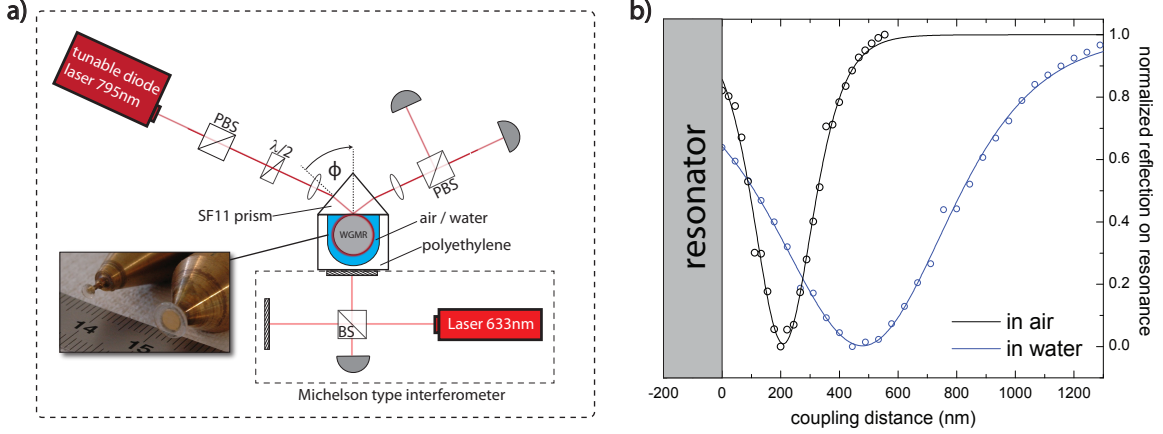


FIG. 2: a) shows the setup used to characterize the two MgF_2 resonators. They can be mounted from above within a basin which itself is mounted onto a piezostage. One of the walls of the basin is a SF11 prism which is used for coupling a tunable laser around 795 nm to TM and TE modes simultaneously by using 45° polarized light. The reflected light is separated via a polarizing beam splitter and sent to two photodiodes to enable tracing of TM and TE spectra at the same time. A mirror which is part of a Michelson type interferometer is attached to the backside of the basin to measure the displacement of the prism with respect to the resonator. The results of this measurement are shown in b): we plot the normalized coupling contrast of two (different) TM modes of the large resonator ($R = 2.91$ mm) in air and water against the traveling distance of the coupling prism. From this we extract the evanescent field decay length for air (water)

$$\kappa^{-1} = 134(382) \text{ nm by fitting equation (4) to the data.}$$

here, λ_0 is the vacuum wavelength and n_{eff} is the effective refractive index of the considered mode, which is always below, but usually close to the bulk refractive index n_r . From this the field decay length in water κ^{-1} can be calculated to be 379 nm for TM in a MgF_2 resonator with $R = 1$ mm and only 231 nm for TM in a fused silica sphere with $R = 0.235$ mm. The radii correspond to resonators of same bulk index sensitivity. Such a long evanescent field extension can be advantageous because the overlap and thus the sensitivity will be enhanced if sensing of large particles or microorganisms like bacteria is desired [20].

III. EXPERIMENT

The experimental setup is depicted in Fig. 2(a). The resonator is glued onto a rigid brass rod which is mounted ‘head down’ such that the resonator is located in a basin which can be water filled. Three of the basin’s walls are made of polyethylene while the fourth is a SF11 glass prism ($n_p \approx 1.77$) which is used for evanescent coupling to the resonator. The light, coming from a widely tunable grating stabilized diode laser emitting around 795 nm, was adjusted to 45° linear polarization to excite TE and TM modes simultaneously. In reflection, the light is separated by a polarizing beamsplitter to discriminate and trace TE and TM modes at the same time. The coupling strength can be adjusted by moving the whole basin and thus the prism via a piezo stage. To investigate the evanescent field decay, we measured the traveling distance of the piezo via a Michelson type interferometer whereby one of the

mirrors is attached to the backside of the basin.

For our experiments, we use two MgF_2 resonators ($n_o = 1.375$, $n_e = 1.387$ at 795 nm) of different size. Both were fabricated on a home build lathe as described in [9]. A diamond cutter was used to preshape the rim of the resonators for optimized incoupling followed by careful hand polishing with a diamond slurry to ensure optical quality of the surface and hence high Q factors. The larger resonator has a radius of $R = 2.91$ mm and the smaller one $R = 1.19$ mm.

Due to the birefringence of MgF_2 , the fundamental TE and TM modes have slightly different coupling angles according to $\phi = \arcsin(n_r/n_p)$ (see Fig. 2(a)) inside the prism. The optimal coupling angles outside the prism hence differ by about 1.1° which is small enough to excite fundamental modes of both polarizations simultaneously with minor loss of coupling efficiency.

Figure 3 shows exemplary overview spectra and Q factor measurements for TM modes of the large resonator in air and in deionized water. Loaded quality factors were derived from sideband calibrated line width measurements at critical coupling according to $Q = \nu/\Delta\nu$. While coupling depth and modal density remain approximately the same when the resonators are immersed in water, the Q factor drops significantly as water has higher absorption than MgF_2 at 795 nm. For TM (TE) we measured $Q_{\text{air}} = 7.3 \times 10^8$ (1.9×10^8) and $Q_{\text{water}} = 2.1 \times 10^8$ (1.7×10^8). The Q factors for the small resonator are slightly smaller, but still remain above 1×10^8 in air and water. Apart from the initial drop, the Q factors were stable over several hours in water.

We investigated the length of the evanescent field by measuring the intensity reflected from the cavity at resonance wavelength for different coupling strengths while also registering the traveling distance of the prism via the interferometer. In Fig. 2(b) such data for the small resonator in air and water environment are plotted for two (different) TM modes: the reflected intensity is normalized such that critical coupling (maximum contrast) corresponds to zero and no coupling to one. The normalized reflected intensity can be described by [27]

$$\Re = \left(\frac{1 - A r e^{-2\kappa d}}{1 + r e^{-2\kappa d}} \right)^2, \quad (4)$$

where A contains the geometrical matching of the incoming beam with the outcoupled one, while $r = \delta_c/\delta_i$ is the ratio between maximally achievable coupling δ_c and intrinsic loss δ_i and d is the distance of the coupler to the resonator's surface. From this fit we derive the field decay lengths $\kappa^{-1} = 134$ nm in air and 382 nm in water which matches the theoretical values of 135 nm and 377 nm quite well. Note that the theoretical values were derived using n_{eff} for the a fundamental mode $q = 1$ and not just the bulk index.

For sensitivity measurements, we filled the basin with a defined amount of deionized water, waited till the thermal equilibrium was reached and readjusted the resonator-prism distance to reach the critical coupling regime again. We prepared a glycerol solution of known concentration and also let it reach equilibrium conditions. For each measurement, 10 μl of the glycerol solution were added to the basin and mixed carefully to prevent the buildup of concentration gradients. After 60 s, when the mode shifts reached equilibrium, both spectra, TE and TM, were acquired via an oscilloscope. The shifts were evaluated by fitting a Lorentzian to each mode and comparing the peak positions between each measurement. We calculate the refractive index change for each measurement from the injected amount of glycerol using the Lorentz-Lorenz relation [12]. The results are presented in Fig. 4 where the wavelength shift of modes of both polarizations from both resonators are plotted against

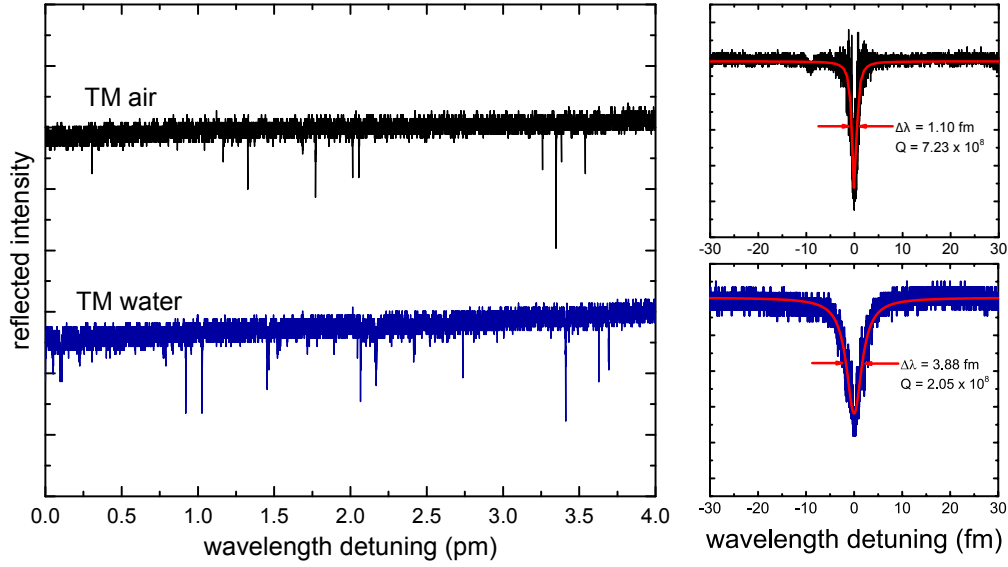


FIG. 3: shows exemplary overview spectra of different TM modes of the large resonator in air and immersed in water after readjusting coupling. Qualitatively, modal density and coupling efficiency remains the same in water. Also shown are zoom ins of (two different) TM modes before and after immersing the resonator. The loaded Q factor was derived from the linewidth acquired by Lorentzian fits while the resonator was critically coupled. The measured linewidth in air was limited by the linewidth of the used laser system.

the refractive index change. As this change is only small, the spectrum's response is as expected for both resonators linear and the sensitivity can be extracted from the slope of a linear fit to each curve.

Qualitatively the curves match the expected behavior: the small resonator is more sensitive to refractive index changes than the larger one and in both resonators the TM mode shifts stronger than the TE mode. The large resonator shows a sensitivity of 1.10 (0.73) nm/RIU for TM (TE) which deviates less than 5% from the theoretical values for $q = 1$ modes. The small resonator, however, shows a sensitivity of 3.26 (2.19) nm/RIU for TM (TE), which is about 15% higher than theory predicts for fundamental modes. In Fig. 4 the theoretically expected responses for the small resonator are represented by the dashed lines and show that the experimental sensitivity exceeds the theoretical one systematically.

IV. CONCLUSION

In this paper, we discuss and demonstrate for the first time the feasibility of high- Q crystalline whispering gallery mode resonators made from magnesium fluoride for refractometric sensing. We show theoretically that MgF_2 with its refractive index being close to that of water and slightly polarization dependent (birefringent) has some advantageous properties over the standard sensing material fused silica. The smaller refractive index leads to stronger interaction with the surrounding medium and thus to better sensitivity, which allows to use larger resonators providing intrinsically larger modal density and better short

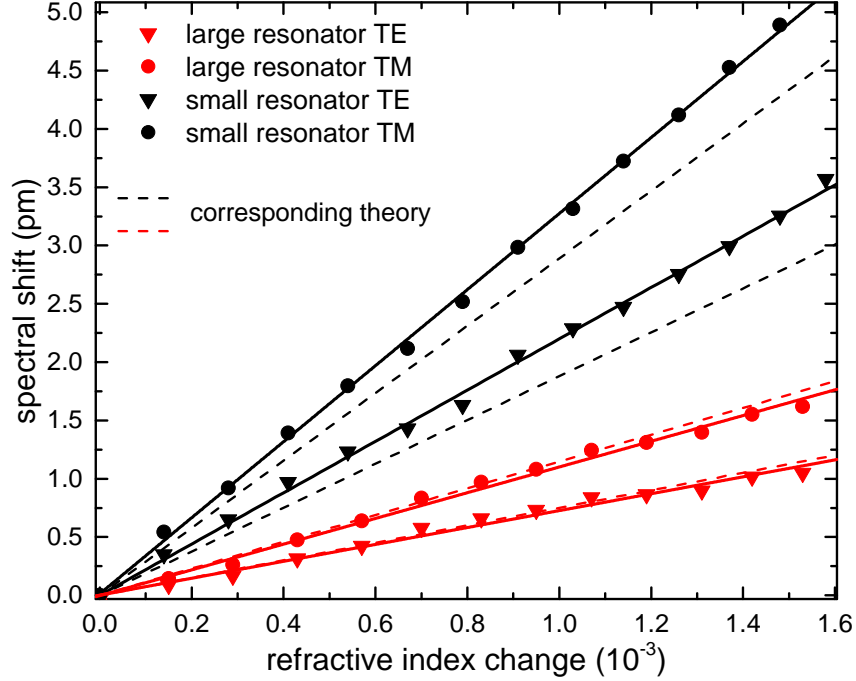


FIG. 4: The plot shows the measured wavelength change of TE and TM modes against refractive index change of the surrounding water for the large ($R = 2.91$ mm) and the small ($R = 1.19$ mm) resonator. Linear fits, indicated by the straight lines, were used to extract the sensitivities. The dashed lines correspond to the expected responses derived from Eqs. (1) and (2) for the different cases. One can see that the sensitivity of the small resonator is about 15% above the theoretically predicted trend.

term stability than a fused silica resonator of same sensitivity. These properties simplify rigid mechanical mounting, the implementation of measurement schemes requiring multiple modes and the tracing of fast processes. The birefringence amplifies the sensitivity difference between TM and TE mode families which is helpful for the implementation of temperature drift neglecting schemes.

We do first experiments, proving that MgF_2 WGM resonators are suitable devices for refractometric applications. Two resonators of different size in the mm regime were fabricated via diamond turning and carefully characterized in air and aqueous environment. In water, both resonators show non decaying loaded Q -factors above 10^8 and keep their high modal density. Using interferometric distance measurements, we show that the penetration depth of the evanescent field matches the theoretical prediction quite well and is thus approximately two times larger than for fused silica resonators of same sensitivity. Finally, the sensitivity dependence on polarization and resonator size is demonstrated by measuring the response of TM and TE modes to small refractive index changes of the water. Here we observe a higher than expected sensitivity for the small resonator. The reason for this is unclear and will be subject of a further study.

Theoretical calculations [17] show that even for the small index difference between MgF_2 and water the radiation limited Q factor remains far above 10^8 for resonator radii smaller than $250\text{ }\mu\text{m}$. This means, according to our calculations and measurements, that MgF_2 resonators can easily compete with fused silica spheres smaller than $60\text{ }\mu\text{m}$, while maintaining the advantages we have pointed out. Furthermore, we recently showed that the slight birefringence of a MgF_2 WGM resonator can harbor elliptically polarized modes if its optic axis is tilted with respect to the rotational symmetry axis while preserving ultrahigh Q factors [23]. This feature could enable sensing of optically active liquids.

V. ACKNOWLEDGEMENTS

We acknowledge fruitful discussions with Martin D. Baaske, Matthew R. Foreman and Frank Vollmer from the Lab of Nanophotonics and Biosensing. We also acknowledge support by Deutsche Forschungsgemeinschaft and Friedrich-Alexander-Universität Erlangen-Nürnberg (FAU) within the funding programme Open Access Publishing.

-
- [1] J. Alnis, A. Schliesser, C. Y Wang, J. Hofer, T. J Kippenberg, and T. W Hänsch. Thermal-noise limited laser stabilization to a crystalline whispering-gallery-mode resonator. *1102.4227*, February 2011. URL <http://arxiv.org/abs/1102.4227>.
 - [2] S. Arnold, M. Khoshshima, I. Teraoka, S. Holler, and F. Vollmer. Shift of whispering-gallery modes in microspheres by protein adsorption. *Opt. Lett.*, 28(4):272–274, February 2003. doi:10.1364/OL.28.000272. URL <http://ol.osa.org/abstract.cfm?URI=ol-28-4-272>.
 - [3] I. Breunig, B. Sturman, F. Sedlmeir, H. G. L. Schwefel, and K. Buse. Whispering gallery modes at the rim of an axisymmetric optical resonator: Analytical versus numerical description and comparison with experiment. *Opt. Express*, 21(25):30683–30692, December 2013. doi:10.1364/OE.21.030683. URL <http://www.opticsexpress.org/abstract.cfm?URI=oe-21-25-30683>.
 - [4] Venkata R. Dantham, Stephen Holler, Curtis Barbre, David Keng, Vasily Kolchenko, and Stephen Arnold. Label-free detection of single protein using a nanoplasmonic-photonic hybrid microcavity. *Nano Lett.*, 13(7):3347–3351, July 2013. ISSN 1530-6984. doi:10.1021/nl401633y. URL <http://dx.doi.org/10.1021/nl401633y>.
 - [5] Yury A. Demchenko and Michael L. Gorodetsky. Analytical estimates of eigenfrequencies, dispersion, and field distribution in whispering gallery resonators. *J. Opt. Soc. Am. B*, 30(11):3056–3063, November 2013. doi:10.1364/JOSAB.30.003056. URL <http://josab.osa.org/abstract.cfm?URI=josab-30-11-3056>.
 - [6] Marilyn J. Dodge. Refractive properties of magnesium fluoride. *Appl. Opt.*, 23(12):1980, June 1984. ISSN 0003-6935, 1539-4522. doi:10.1364/AO.23.001980. URL <http://www.opticsinfobase.org/ao/fulltext.cfm?uri=ao-23-12-1980&id=27584>.
 - [7] Michael L. Gorodetsky and Ivan S. Grudinin. Fundamental thermal fluctuations in microspheres. *J. Opt. Soc. Am. B*, 21(4):697–705, April 2004. doi:10.1364/JOSAB.21.000697. URL <http://josab.osa.org/abstract.cfm?URI=josab-21-4-697>.
 - [8] M.L. Gorodetsky and A.E. Fomin. Geometrical theory of whispering-gallery modes. *IEEE J. Sel. Top. Quant. Electron.*, 12(1):33–39, 2006. ISSN 1077-260X. doi:10.1109/JSTQE.2005.862954. URL 10.1109/JSTQE.2005.862954.

- [9] Ivan S. Grudinin, Vladimir S. Ilchenko, and Lute Maleki. Ultrahigh optical Q factors of crystalline resonators in the linear regime. *Phys. Rev. A*, 74(6):063806, December 2006. doi:10.1103/PhysRevA.74.063806. URL <http://link.aps.org/doi/10.1103/PhysRevA.74.063806>.
- [10] Guoming Guan, Stephen Arnold, and Volkan Otugen. Temperature measurements using a microoptical sensor based on whispering gallery modes. *AIAA Journal*, 44(10):2385–2389, 2006. ISSN 0001-1452. doi:10.2514/1.20910. URL <http://arc.aiaa.org/doi/abs/10.2514/1.20910>.
- [11] Niranjana M. Hanumegowda, Caleb J. Stica, Bijal C. Patel, Ian White, and Xudong Fan. Refractometric sensors based on microsphere resonators. *Appl. Phys. Lett.*, 87(20):201107–201107–3, 2005. ISSN 0003-6951. doi:10.1063/1.2132076.
- [12] Jose V. Herráez and R. Belda. Refractive indices, densities and excess molar volumes of monoalcohols + water. *J. Solution Chem.*, 35(9):1315–1328, September 2006. ISSN 0095-9782, 1572-8927. doi:10.1007/s10953-006-9059-4. URL <http://link.springer.com/article/10.1007/s10953-006-9059-4>.
- [13] Heather K. Hunt, Carol Soteropulos, and Andrea M. Armani. Bioconjugation strategies for microtoroidal optical resonators. *Sensors*, 10(10):9317–9336, October 2010. doi:10.3390/s101009317. URL <http://www.mdpi.com/1424-8220/10/10/9317>.
- [14] Tindaro Ioppolo, Michael Kozhevnikov, Vadim Stepaniuk, M. Volkan Ötügen, and Valery Sheverev. Micro-optical force sensor concept based on whispering gallery mode resonators. *Appl. Opt.*, 47(16):3009–3014, June 2008. doi:10.1364/AO.47.003009. URL <http://ao.osa.org/abstract.cfm?URI=ao-47-16-3009>.
- [15] Thanh Le, Anatoliy Savchenkov, Nan Yu, Lute Maleki, and W. H. Steier. Optical resonant sensors: a method to reduce the effect of thermal drift. *Appl. Opt.*, 48(3):458–463, January 2009. doi:10.1364/AO.48.000458. URL <http://ao.osa.org/abstract.cfm?URI=ao-48-3-458>.
- [16] W. Liang, A. A. Savchenkov, A. B. Matsko, V. S. Ilchenko, D. Seidel, and L. Maleki. Generation of near-infrared frequency combs from a MgF₂ whispering gallery mode resonator. *Optics Letters*, 36(12):2290–2292, June 2011. doi:10.1364/OL.36.002290. URL <http://ol.osa.org/abstract.cfm?URI=ol-36-12-2290>.
- [17] B.E. Little, J.-P. Laine, and H.A. Haus. Analytic theory of coupling from tapered fibers and half-blocks into microsphere resonators. *J. Lightwave Technol.*, 17(4):704–715, 1999. ISSN 0733-8724. doi:10.1109/50.754802. URL 10.1109/50.754802.
- [18] Julie Lutti, Wolfgang Langbein, and Paola Borri. A monolithic optical sensor based on whispering-gallery modes in polystyrene microspheres. *Appl. Phys. Lett.*, 93(15):151103, 2008. ISSN 00036951. doi:10.1063/1.2998652. URL <http://orca.cf.ac.uk/9041/>.
- [19] Anatolii N Oraevsky. Whispering-gallery waves. *Quant. Electron.*, 32(5):377–400, May 2002. ISSN 1063-7818. doi:10.1070/QE2002v032n05ABEH002205. URL http://www.turpion.org/php/paper.phtml?journal_id=qe&paper_id=2205.
- [20] Hai-Cang Ren, Frank Vollmer, Stephen Arnold, and Albert Libchaber. High-Q microsphere biosensor - analysis for adsorption of rodlike bacteria. *Opt. Express*, 15(25):17410–17423, December 2007. ISSN 1094-4087. PMID: 19551035.
- [21] Anatoliy A. Savchenkov, Andrey B. Matsko, Vladimir S. Ilchenko, Nan Yu, and Lute Maleki. Whispering-gallery-mode resonators as frequency references. II. stabilization. *J. Opt. Soc. Am. B*, 24(12):2988–2997, December 2007. doi:10.1364/JOSAB.24.002988. URL <http://josab.osa.org/abstract.cfm?URI=josab-24-12-2988>.

- [22] Stephan Schiller and R. L. Byer. High-resolution spectroscopy of whispering gallery modes in large dielectric spheres. *Opt. Lett.*, 16(15):1138–1140, August 1991. doi:10.1364/OL.16.001138. URL <http://ol.osa.org/abstract.cfm?URI=ol-16-15-1138>.
- [23] Florian Sedlmeir, Martin Hauer, Josef U. Fürst, Gerd Leuchs, and Harald G. L. Schwefel. Experimental characterization of an uniaxial angle cut whispering gallery mode resonator. *Optics Express*, 21(20):23942–23949, October 2013. doi:10.1364/OE.21.023942. URL <http://www.opticsexpress.org/abstract.cfm?URI=oe-21-20-23942>.
- [24] H. Tavernier, P. Salzenstein, K. Volyanskiy, Y.K. Chembo, and L. Larger. Magnesium fluoride whispering gallery mode disk-resonators for microwave photonics applications. *IEEE Photonics Technology Letters*, 22(22):1629–1631, November 2010. ISSN 1041-1135. doi:10.1109/LPT.2010.2075923.
- [25] F. Vollmer, S. Arnold, and D. Keng. Single virus detection from the reactive shift of a whispering-gallery mode. *Proc. Natl. Acad. Sci. U.S.A.*, 105(52):20701–20704, December 2008. ISSN 0027-8424, 1091-6490. doi:10.1073/pnas.0808988106. URL <http://www.pnas.org/content/105/52/20701>. PMID: 19075225.
- [26] Frank Vollmer and Stephen Arnold. Whispering-gallery-mode biosensing: label-free detection down to single molecules. *Nat. Methods*, 5(7):591–596, July 2008. ISSN 1548-7091. doi:10.1038/nmeth.1221. URL <http://www.nature.com/nmeth/journal/v5/n7/abs/nmeth.1221.html>.
- [27] S. P. Vyatchanin, M. L. Gorodetskii, and V. S. Il’chenko. Tunable narrow-band optical filters with modes of the whispering gallery type. *J. Appl. Spectrosc.*, 56(2):182–187, February 1992. ISSN 0021-9037, 1573-8647. doi:10.1007/BF00662275. URL <http://link.springer.com/article/10.1007/BF00662275>.
- [28] T. Weigel, C. Esen, G. Schweiger, and A. Ostendorf. Whispering gallery mode pressure sensing. *Proc. SPIE*, 8439:84390T–84390T–6, 2012. doi:10.1117/12.921759. URL <http://dx.doi.org/10.1117/12.921759>.
- [29] Vanessa Zamora, Antonio Díez, Miguel V. Andrés, and Benito Gimeno. Refractometric sensor based on whispering-gallery modes of thin capillaries. *Opt. Express*, 15(19):12011–12016, September 2007. doi:10.1364/OE.15.012011. URL <http://www.opticsexpress.org/abstract.cfm?URI=oe-15-19-12011>.